COVID-19 and surface water quality: Improved lake water quality during the lockdown

Ali P. Yunus [a,b,*], Yoshifumi Masago [b], Yasuaki Hijioka [b]

[a] State Key Laboratory for Geohazard Prevention and Geoenvironment Protection, Chengdu University of Technology, Chengdu, Sichuan 610059, China
[b] Center for Climate Change Adaptation, National Institute for Environmental Studies, Tsukuba, Ibaraki 305-8506, Japan

HIGHLIGHTS

- First attempt to track the impact of the COVID-19 spread on the hydrosphere.
- Business lockdown due to the COVID-19 spread improved adjacent lake water quality.
- Suspended particular matter concentration in Vembanad lake decreased by 15.9%.
- Eleven out of 20 zones showed the lowest April SPM in 2020.
- Business activities have a significant impact on the lake water quality.

GRAPHICAL ABSTRACT
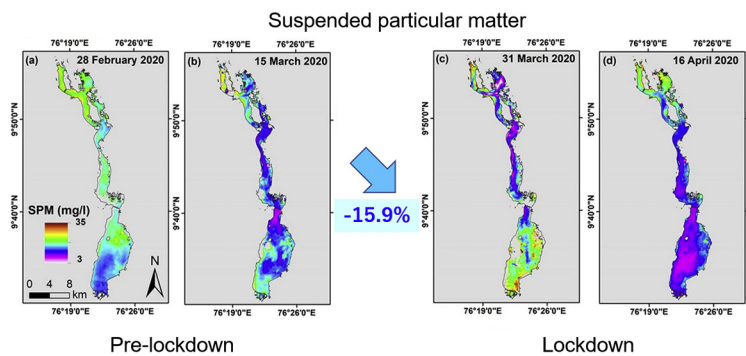
ABSTRACT

Human life comes to a standstill as many countries shut themselves off from the work due to the novel corona-virus disease pandemic (COVID-19) that hit the world severely in the first quarter of 2020. All types of industries, vehicle movement, and people's activity suddenly halted, perhaps for the first time in modern history. For a long time, it has been stated in various literature that the increased industrialization and anthropogenic activities in the last two decades polluted the atmosphere, hydrosphere, and biosphere. Since the industries and people's activities have been shut off for a month or more in many parts of the world, it is expected to show some improvement in the prevailing conditions in the aforementioned spheres of environment. Here, with the help of remote sensing images, this work quantitatively demonstrated the improvement in surface water quality in terms of suspended particulate matter (SPM) in the Vembanad Lake, the longest freshwater lake in India. The SPM estimated based on established turbidity algorithm from Landsat-8 OLI images showed that the SPM concentration during the lockdown period decreased by 15.9% on average (range: −10.3% to 36.4%, up to 8 mg/l decrease) compared with the pre-lockdown period. Time series analysis of satellite image collections (April 2013 – April 2020) showed that the SPM quantified for April 2020 is the lowest for 11 out of 20 zones of the Vembanad lake. When compared with preceding years, the percentage decrease in SPM for April 2020 is up to 34% from the previous minima.

* Corresponding author at: State Key Laboratory for Geohazard Prevention and Geoenvironment Protection, Chengdu University of Technology, Chengdu, Sichuan 610059, China.
E-mail address: pulpadan.yunusali@nies.go.jp (A.P. Yunus).

1. Introduction

As of mid-April 2020, the disease caused by severe acute respiratory syndrome coronavirus 2 (SARS-CoV-2) is affecting about 210 countries and territories around the world (Worldometers.info 2020). Over 2 million cases of virus infection were reported all over the globe, with most fatalities reported in the United States of America, Spain, and Italy. Originated initially in December 2019 in Wuhan, China, the coronavirus disease 2019 (COVID-19) spread swiftly from person to person from respiratory droplets when an infected person coughs, sneezes, or talks. Or, it spread by touching a surface or object that has the virus on it, and then by touching the mouth, nose, or eyes. Since there is no vaccine or medicine currently to prevent or cure the COVID-19, the World Health Organization and governmental bodies requested people for practicing social distance, avoid public transportation, and separate oneself from other people. Several countries and territories made swift and stern action to keep people stay at their homes by shutting down schools, industries, businesses, suspended travels, and closed the international and state boundaries. Normal life has come to a standstill around the globe since February 2020.

It is stated and proved in several studies that anthropogenic activities are considered as one of the key drivers of pollution in all spheres of the environment (Akimoto 2003; Volkamer et al. 2006; Masood et al. 2016; Schlacher et al. 2016). Since people's movements and industrial activities are closed down for weeks, it is expected that pollution loads to the environment also get decreased. As expected, in a matter of days, the carbon emissions level has dropped significantly (Stone 2020). According to the Ministry of Ecology and Environment, China, the air quality went up 11% in the category 'good' in as many as 337 cities (Henriques 2020). Scripps Institute of Oceanography reported that the use of fossil fuel would decline by about 10% around the world owing to the COVID-19 spread (SCRIPPS 2020). While these improvements in environmental pollution are considered to be temporary, the current level of pollution in the atmosphere, biosphere, and hydrosphere could be much lower than the pre-COVID-19 period.

Quantifying the status of pollution during the lockdown period is an important task for researchers to understand the effect of the COVID-19 spread on the environment in the short- and long-term. Satellite-based data from Tropospheric Monitoring Instrument (TROPOMI) on ESA's Sentinel-5 satellite and the Ozone Monitoring Instrument (OMI) on NASA's Aura satellite shows a decreased level of nitrogen dioxide (NO_2) in the atmosphere (ESA 2020). On the other hand, the status of pollution in the hydrosphere that includes lakes, rivers, oceans, and groundwater reservoirs, has not been investigated. For decades, the hydrosphere has been severely polluted because of rapid urbanization, industrialization, and overexploitation. During the lockdown period, the major industrial sources of pollution that affect aquatic ecosystems, such as industrial wastewater disposal, crude oil, heavy metals, and plastics (Häder et al. 2020), have shrunk or completely stopped. Therefore, the level of pollution is expected to be reduced. For example, news media reported that the Grand Canal in Italy, where the COVID-19 crippled the whole nation, turned clear, and reappearances of many aquatic species (Clifford 2020). Similarly, the Ganges, a sacred but severely polluted river in India, turns cleaner at several places during the nationwide lockdown period that started on 25th March 2020 (Mani 2020).

This study made a first attempt to quantify the level of ambient water pollution during the COVID-19 spread. The objective of the study is to analyze the status of water pollution in Vembanad Lake, the longest freshwater lake in India, and to evaluate the effect of the lockdown on the water quality. Turbidity, determined by remote sensing technology, was selected as an indicator of water pollution (Stumpf and Pennock 1989).

2. Study area

Vembanad Lake is selected as a case area to study water quality before and during the COVID-19 lockdown period. The study area forms a part of the Vembanad wetland system, a recognized Ramsar site, located in the state of Kerala, between 9.9545° N - 9.5214° N latitudes and 76.2105° E - 76.5430° E longitudes (Fig. 1). The lake area covers approximately 250 km^2 and its catchment area including seven small river basins covers >14,000 km^2 (Padmalal et al. 2008). The lake is one of the famous scenic attractions in the state. It has also been served as a livelihood for the local population in the form of tourism and aquaculture being the main income source. The lake is polluted severely - the abundance of microplastics recorded from the sediment samples is as high as 496 particles m^{-2} (Sruthy and Ramasamy 2017). High concentrations of toxic elements such as mercury are reported from surface and subsurface sediment samples, as well as from fish samples (Mohan et al. 2014; Ramasamy et al. 2017). The spatial variation of the pollutants indicates that industrial effluents are the major source of pollution in the Vembanad lagoon system (Priju and Narayana 2007).

The first case of COVID-19 reported in the state of Kerala is in the late January 2020, and the state undergoes lockdown on 25th March 2020 together with the other states of India after the Prime Minister declared the emergency on the night of 24th March 2020. However, the normal businesses around the lake such as tourism were affected much before 21st March because several positive imported cases were reported in various parts of the state. Since the industries and tourism activities (houseboats which run on diesel engines) have closed down completely after 25th March 2020, the pollution from these sources has almost halted, which made Vembanad lake a unique opportunity to study the effect of the lockdown on water quality.

3. Materials and methods

3.1. Theoretical background

While the turbidity cannot be a sole indicator of water quality, it has been used to assess overall water quality (Woodruff et al. 1999; Davies-Colley and Smith 2001; Luis et al. 2019). Suspended particulate matter (SPM) caused by sedimentation, siltation, sewage disposal, other pollutants, metals, and bacteria results in high turbidity in aquatic environments. In the earliest literature, a Secchi disk was used to measure water transparency or turbidity. However, field-based methods have inherent limitations in spatial coverage because of the time and cost of observation. With the advent of remote sensing techniques, researchers investigated the relationship between turbidity and reflectance in waters bodies (Curran et al. 1987; Novo et al. 1989). The results of these studies are promising and showed that reflectance increases with increasing turbidity. For instance, Doxaran et al. (2002) concluded that reflectance between 400 and 1000 nm increases with turbidity, in particular, when the turbidity level is 35 to 250 mg/l, the reflectance between 400 and 700 nm correlates well with the turbidity. Several empirical calibrated models have been developed using linear, log-linear, non-linear, and exponential relationship with reflectance products from satellite images in the visible spectrum (Dogliotti et al. 2015; Doxaran et al. 2003; Nechad et al. 2010; Song et al. 2011; Sravanthi et al. 2013; Tassan 1994; Wass et al. 1997). With a large number of optical satellite sensor orbiting the earth, mapping of turbidity in aquatic environments in the form of surface SPM or total suspended matter (TSM) has been widely conducted using Landsat, Spot, SeaWiFS, MERIS, MODIS Aqua and Terra, OceanSAT, Sentinel-2, and recently released Sentinel-3 OLCI images (e.g., Ritchie et al. 1990; Tassan 1994; Vanhellemont and Ruddick 2014; Wei et al. 2018). In this study, high-resolution Landsat 8 OLI imagery between
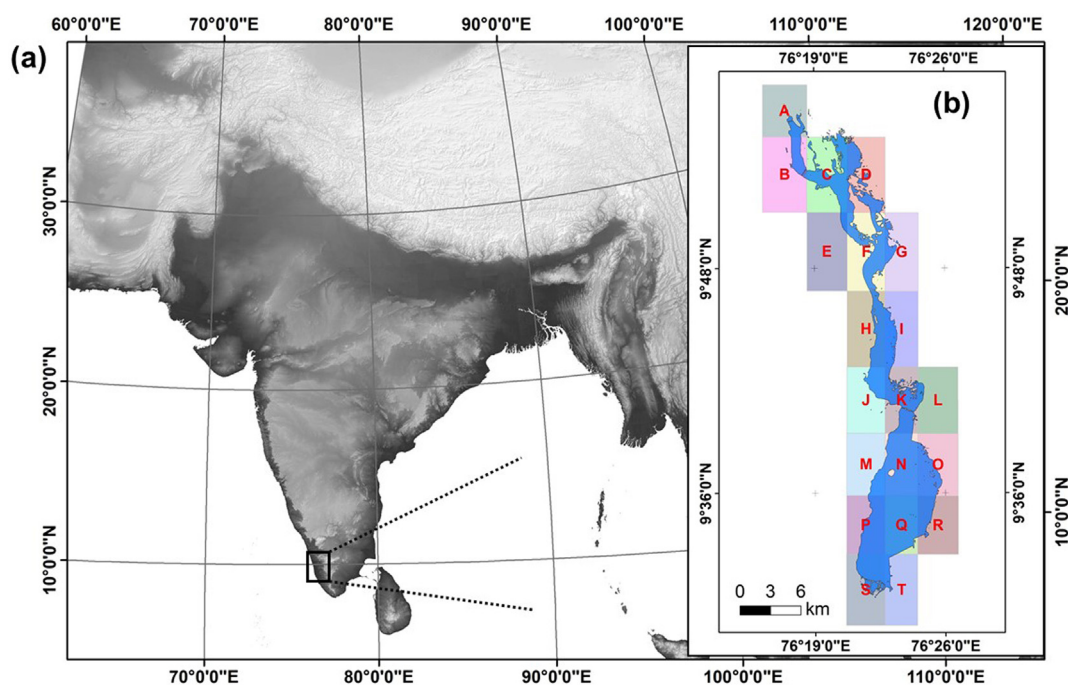
Fig. 1. (a) location map of the study area, (b) Vembanad lake boundary, and demarcation of different zones (A – T) used for quantifying the mean suspended particulate matter.

April 2013 and April 2020 was obtained and analyzed using an established SPM algorithm (Nechad et al. 2010).

3.2. Acquisition of landsat-8 operational land imager (OLI) and pre-processing

Eleven Landsat 8 OLI images (Path/Row: 144/53) of Vembanad Lake, from April 2013 to April 2020, were downloaded (Table 1) from the United States Geological Survey (USGS) website (earthexplorer.usgs.gov). All the downloaded scenes were level-1 processed, meaning that they underwent correction for terrain geo-registration within prescribed tolerances (<12 m root mean square error (RMSE)). The level-1 terrain corrected images were processed in two steps: 1) radiometric calibration for obtaining Top of Atmosphere (ToA) Reflectance, and 2) atmospheric correction for obtaining surface reflectance products.

ACOLITE software environment developed at Royal Belgian Institute of Natural Science is used for pre-processing the Landsat-8 OLI imagery. ACOLITE allows quick processing of high-resolution satellite images for coastal and inland water applications. It performs first conversion of raw digital numbers (DN) to radiance values (using gain and bias values), then converts these radiance values to ToA reflectance values (using distance between the sun and earth in astronomical units, Julian date, and solar zenith angle). Next, it performs the atmospheric correction using the "dark spectrum fitting" (DSF) approach (Vanhellemont and Ruddick 2018; Vanhellemont 2019). Several previous studies have successfully utilized the calibrated results from ACOLITE model for estimating suspended sediments, measuring bathymetry, and chlorophyll-a in inland and ocean interfaces (e.g., Caballero and Stumpf 2019).

The DSF model uses atmospheric path reflectance of multiple dark targets in the scene or subscene. A continental or maritime aerosol model can be chosen based on the lowest root mean square (RMS) difference between the observed dark spectrum and the retrieved path reflectance for the two closest fitting bands. A combination of the NIR (0.8 μm) and Short Wave Infrared (1.6 μm) channels are used for atmospheric correction in ACOLITE. For moderate turbid environments, this combination strategy has been proved successful (Pahlevan et al. 2017).

3.3. SPM algorithm

In a previous field campaign, Sravanthi et al. (2013) measured in situ SPM at the mouth of the lake-estuarine system of Vembanad, and reported that it was in the range of 14–33 mg/l during October to February months. In another study, Vinita et al. (2017) showed that the in situ SPM measured in the lake ranged between 20 mg/l (wet season minimum) and 101 mg/l (dry season maximum). Both aforementioned studies suggested that the turbidity level in the lake is <110 mg/l throughout the year. Nechad et al. (2010) proposed a single band empirical algorithm to retrieve the SPM concentrations for waters where SPM value is below the range of 110 mg/l. Considering both analyses reported a similar range of turbidity, it is safe to assume that applying the Nechad et al. (2010) empirical model can retrieve SPM with an RMS error of <10 mg/l.

Table 1
Landsat-8 OLI images (Path 144 – Row 53) of the Vembanad lake used in this study.

Date of image acquisition	Product ID	Remarks
2013-04-13	LC08_L1TP_144053_20130413_20170505_01_T1	–
2014-04-16	LC08_L1TP_144053_20140416_20170423_01_T1	–
2015-04-19	LC08_L1TP_144053_20150419_20170409_01_T1	–
2016-04-05	LC08_L1TP_144053_20160405_20170327_01_T1	–
2017-04-08	LC08_L1TP_144053_20170408_20170414_01_T1	–
2018-04-27	LC08_L1TP_144053_20180427_20180502_01_T1	–
2019-04-14	LC08_L1TP_144053_20190414_20190422_01_T1	–
2020-02-28	LC08_L1TP_144053_20200228_20200313_01_T1	–
2020-03-15	LC08_L1TP_144053_20200315_20200325_01_T1	–
2020-03-31	LC08_L1TP_144053_20200331_20200410_01_T1	Lockdown period
2020-04-16	LC08_L1TP_144053_20200416_20200416_01_RT	Lockdown period

The SPM is computed from water-leaving reflectance (Rrs) of the red band (655 nm) using the following equation (Nechad et al. 2010):

$$SPM = \frac{A\rho_W}{(1-\rho_W)/C}$$

where ρ_W is Rrs from the red band (655 nm), A and C are empirical coefficients: A = 289.29 and C = 0.1686.

4. Results

Fig. 2 shows the temporal variation of SPM concentrations in Vembanad lake water on 28th February, 15th and 31st March, and 16th April of 2020. Visual interpretation of Fig. 2 clearly shows a decrease in SPM concentration during the lockdown period. For quantitative verification, the lake area was divided into 20 zones (see Fig. 1). Eighteen out of the 20 zones showed a decrease in the SPM concentration, showing that the decrease was observed in the almost entire lake. Comparing the average SPM concentrations of the period of lockdown (31st March and 16th April) with those of the pre-lockdown period (28th February and 15th March), a significant decrease in SPM concentrations was observed (15.9% on average; range: −10.3–36.4%) (Table 2). The mean values of SPM in each zone decreased to a maximum of 8 mg/l.

One can argue that the decrease in SPM concentrations can be attributed to the inter-monthly variation in the suspended loads from the 7 small rivers in the lake catchment. In order to nullify the effect of inter-monthly variation, time-series SPM analysis for images from April 2013 (Landsat-8 OLI launched in 2013) to April 2020 was conducted. Altogether, eight Landsat scenes are available for the time series analysis; the results are presented in Fig. 3.

Time series trend estimated from archived OLI images for April 2013 – April 2020 showed that the SPM concentration was the lowest in April 2020 in 11 zones (Zone F, G, H, I, J, K, M, N, P, Q, S) (Fig. 3 and Fig. A1). On the other hand, the northern zones (A–E) located close to the mouth of the Vembanad lake opening to the Arabian Sea recorded the lowest SPM concentrations in previous years (e.g. 2016). A possible explanation is that seawater intrusion into the lake during the high tide condition, which

Table 2
Mean SPM concentrations in different zones (see Fig. 1) of Vembanad lake in 2020.

Zone	Mean SPM (mg/l)						% Decrease (pre- and during lockdown)
	Pre-lockdown			During lockdown			
	28th February 2020	15th March 2020	Average	31st March 2020	16th April 2020	Average	
A	20.2	18.9	19.5	17.2	23.0	20.1	−3.0
B	20.4	20.4	20.4	14.4	18.9	16.7	18.3
C	19.6	15.9	17.8	11.5	17.4	14.4	18.8
D	17.4	13.4	15.4	10.6	16.9	13.7	11.0
E	20.0	15.5	17.8	10.5	12.1	11.3	36.4
F	16.2	11.7	13.9	10.4	11.9	11.1	20.1
G	15.2	11.7	13.4	11.5	12.0	11.8	12.4
H	16.4	11.3	13.9	10.2	10.0	10.1	27.4
I	16.8	11.8	14.3	11.6	11.6	11.6	18.9
J	16.4	13.8	15.1	11.5	9.4	10.4	30.8
K	16.1	10.7	13.4	11.5	10.6	11.0	17.6
L	16.8	14.0	15.4	14.2	14.3	14.2	7.5
M	15.6	15.0	15.3	15.9	9.8	12.8	16.1
N	16.7	11.6	14.1	13.1	9.3	11.2	20.9
O	17.0	14.2	15.6	16.2	12.3	14.3	8.4
P	13.0	14.0	13.5	14.1	8.4	11.2	16.8
Q	13.5	12.3	12.9	14.0	8.6	11.3	12.5
R	13.7	12.9	13.3	14.5	11.6	13.1	1.9
S	12.2	15.9	14.0	15.9	9.9	12.9	8.2
T	12.0	15.1	13.5	18.1	11.6	14.9	−10.3
All zones	15.8	13.1	14.4	12.7	11.6	12.1	15.9

is typical in this region, could alter the original state of lake biophysical parameters at the closest points to the mouth. Balchand and Nair (1994) reported that saline water intrusion from the Arabian Sea to the Vembanad lake is as much as 26 km from the bar mouth during the pre-monsoon period, both at surface and subsurface levels. Thus, variation in SPM concertation even when the industrial activities are shut is possible at A–E. Further, zones L, O, R and T also recorded their lowest SPM concentration not in 2020, possibly because of their closeness to the river mouths on the south-eastern margin. The percentage decrease in SPM tabulated for April 2020 is, up to 34% from the previous minima (Table A1).
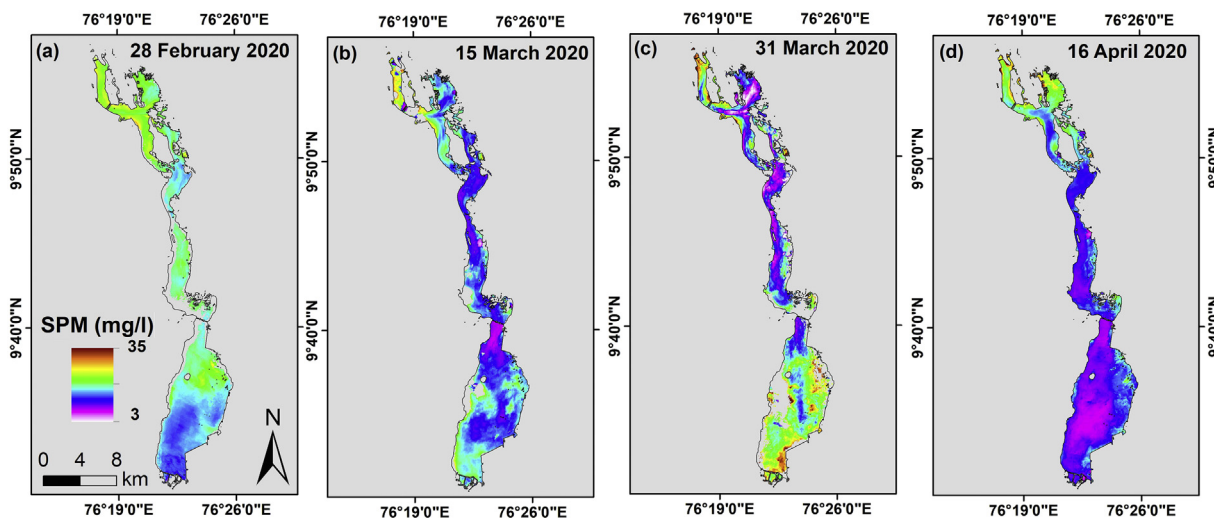

Fig. 2. Suspended particulate matter (SPM) concentrations estimated for the Vembanad lake on 28th February, 15th and 31st March, and 16th April 2020 (values in mg/l; violet is low and dark red is the highest concentration).
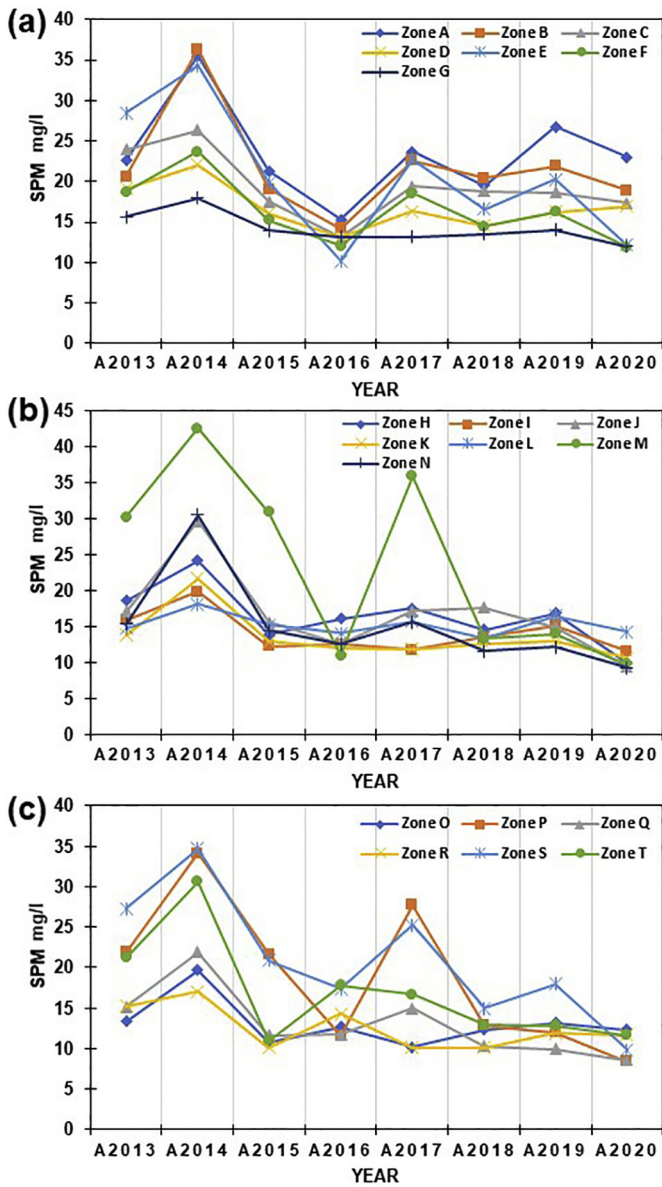
Fig. 3. Time series analysis of suspended particulate matter concentrations in Vembanad lake during April (2013–2020). a) Zone A–G, b) Zone H–N, and c) Zone O–T (refer Fig. 1 for zone identification).

5. Discussion and concluding remarks

The authors attempted to understand the effect of COVID-19 spread in a hydrosphere using remote sensing data products. We selected one of the severely polluted freshwater lakes in India to evaluate the impact of the lockdown due to the COVID-19 spread on water quality. The analysis of SPM concentrations in Vembanad lake based on the Landsat-8 OLI data revealed that the concentrations during the lockdown period were lower than those in the pre-lockdown period by 15.9% on average (−10.3%–36.4%). The decrease was observed in 18 out of 20 zones of the lake. Eleven of the zones showed that the concentration was the lowest in April of 2013–2020 (Table A1). While non-industrial pollution (e.g. discharge of domestic wastewater) remained during the lockdown period, our results suggested that pollution from industries and

tourism had a severe impact on lake water quality. As we have limited satellite data during the lockdown period, further analysis using longer time-series data that include the post-lockdown period (presumably starting from 3rd May 2020) is needed to confirm the effect of industrial pollution load on lake water quality. Another potential extension of this work is to apply MODIS Terra 250 m archived data to derive the time series SPM that dates back to the year 2000. One of the advantages of the remote-sensing-based water quality analysis (over on-site observation) is that we can evaluate past water quality as long as cloud-free satellite images are available. We recommend similar works in other environmental settings to understand the overall impact of COVID-19 in the hydrosphere.

Since the atmospheric components and hydrosphere are closely linked, we also tracked the weather data and atmospheric pollution level in the study region. The atmospheric pollution ($PM_{2.5}$, PM_{10}, and NO_2) data for the study area obtained from the central and state pollution control board showed that the air quality was drastically improved since the first day of the lockdown (Fig. A2b). While the climatic condition in April 2020 was not different from those in other years (Fig. A2a), the particulate matter concentrations (both $PM_{2.5}$ and PM_{10}) in April 2020 was much lower than those in 2019, suggesting a considerable improvement in the pollution level during the lockdown (Fig. A2c). Although associating atmospheric particulate matter with suspended particulate matter in the lake is premature at this point, the improvement in environmental quality was observed in both atmosphere and hydrosphere.

Our findings also draw further attention to what will happen after the lockdown period. The lake is surrounded by densely populated areas (810 inhabitants/km^2) (Narayanan and Venot 2009). The industries, tourism activities, and other businesses (e.g. hotels and restaurants) are planned to re-open in a phased manner from 3rd May 2020. Although the socio-economic effect of COVID-19 spread will remain for some period, the pollutants eventually return to the lake from the industrial activities. Declared as a location of international importance under the Ramsar Convention, also located in the coastal zone, there are rules and regulations formulated to preserve the Vembanad lake ecosystem. But it seems less action being taken on the ground level. Our work showed that the pollutant level decreased considerably when industries and boating being suspended. Therefore, now is the time to take stipulated actions based on the framework of the Ramsar Convention to reduce the environmental damage to the Vembanad lake ecosystem. The sustainable solution has to be reached considering the big tourism economy in the region.

CRediT authorship contribution statement

Ali P. Yunus: Conceptualization, Methodology, Formal analysis, Writing - original draft. **Yoshifumi Masago:** Supervision, Writing - review & editing, Funding acquisition. **Yasuaki Hijioka:** Writing - review & editing, Funding acquisition.

Declaration of competing interest

The authors declared that they have no conflicts of interest to this work.
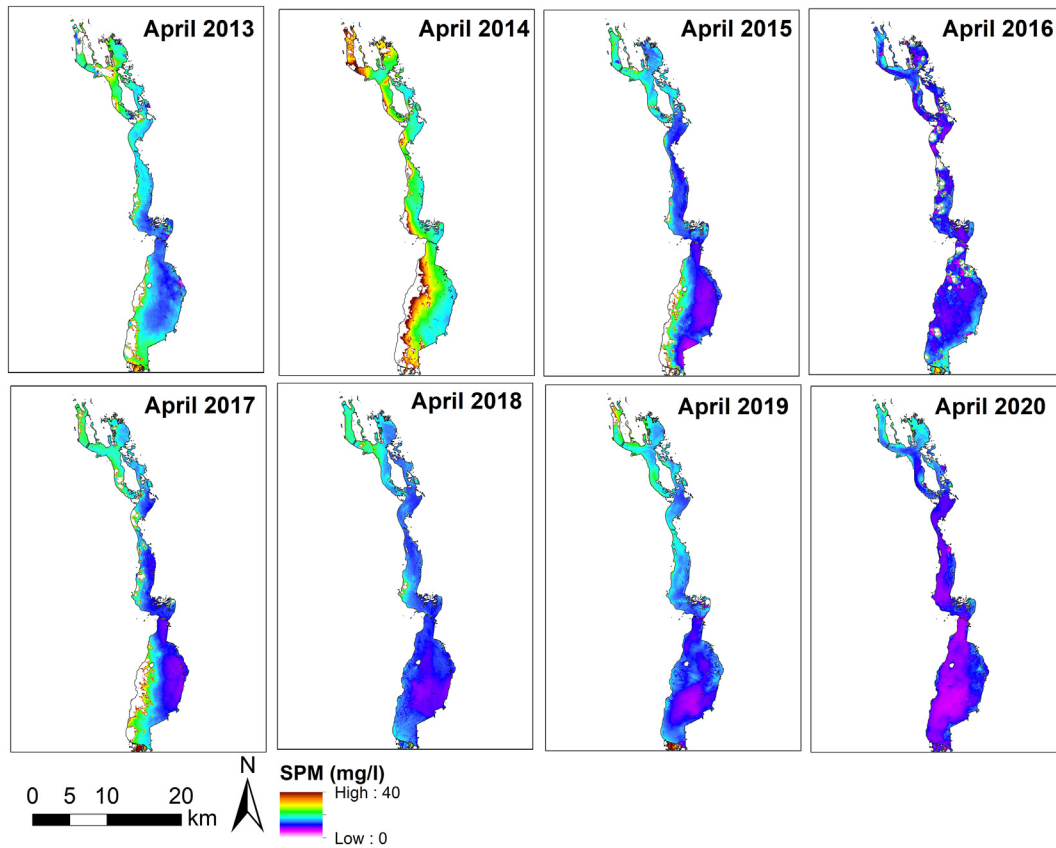
Acknowledgments

Appendix A

Fig. A1. Time series suspended particulate concentrations (2013–2020) estimated for the Vembanad lake.

Table A1
Tabulated SPM Concentrations for April (2013–2020) and percentage decrease in April 2020 from the observed minima and average of the previous years.

| Zone	April 2013	April 2014	April 2015	April 2016	April 2017	April 2018	April 2019	April 2020	Min.& (Avg) of 2013–2019	% decrease (Min. & (Avg.))
A	22.7	35.47	21.31	15.28	23.71	19.46	26.78	23.03	15.2 (23.5)	−50.7 (2.1)
B	20.63	36.3	19.09	14.17	22.56	20.43	21.88	18.94	14.1 (22.2)	−33.6 (14.5)
C	23.94	26.33	17.57	13.11	19.44	18.81	18.61	17.35	13.1 (19.7)	−32.3 (11.9)
D	19.15	22.07	16.08	13.21	16.35	14.59	16.25	16.91	13.2 (16.8)	−28.0 (−0.6)
E	28.46	34.25	19.93	10.22	22.76	16.57	20.26	12.13	10.2 (21.8)	−18.7 (44.3)
F	18.75	23.65	15.19	12.02	18.54	14.47	16.25	11.91	12.0 (17.0)	0.9 (29.9)
G	15.64	17.97	13.91	13.21	13.22	13.51	14.01	11.98	13.2 (14.5)	9.3 (17.4)
H	18.6	24.14	13.91	16.11	17.57	14.56	16.88	9.99	13.9 (17.4)	28.1 (42.6)
I	15.9	19.89	12.24	12.52	11.78	13.53	15.15	11.58	11.7 (14.4)	1.7 (19.8)
J	17.1	29.64	15.67	12.64	17.17	17.64	14.93	9.42	12.6 (17.8)	25.5 (47.2)
K	13.79	21.67	12.94	11.94	11.9	12.7	12.98	10.61	11.9 (14.0)	10.9 (24.2)
L	14.79	18.11	15.23	14.08	15.68	13.42	16.52	14.25	13.4 (15.4)	−6.2 (7.5)
M	30.25	42.56	30.9	11.02	35.93	13.3	13.98	9.79	11.0 (25.4)	11.2 (61.5)
N	15.34	30.58	14.53	12.58	15.67	11.62	12.13	9.26	11.6 (16.1)	20.27 (42.4)
O	13.31	19.69	10.81	12.63	10.19	12.28	13.14	12.3	10.1 (13.2)	−20.7 (6.5)
P	21.89	34.14	21.63	11.53	27.74	12.86	11.97	8.4	11.5 (20.3)	27.14 (58.5)
Q	15.14	21.91	11.63	11.7	14.96	10.28	9.9	8.6	9.9 (13.6)	13.2 (37.0)
R	15.22	17.04	10.14	14.31	10.1	10.12	11.93	11.62	10.1 (12.7)	−15.0 (8.5)
S	27.26	34.67	20.86	17.35	25.19	14.97	17.93	9.87	14.9 (22.6)	34.0 (56.3)
T	21.17	30.58	10.98	17.81	16.72	12.91	12.84	11.62	10.9 (17.6)	−5.8 (33.9)
All zones	17.85	25.18	14.98	13	16.73	13.72	14.44	11.66	13.0 (16.6)	10.3 (29.6)
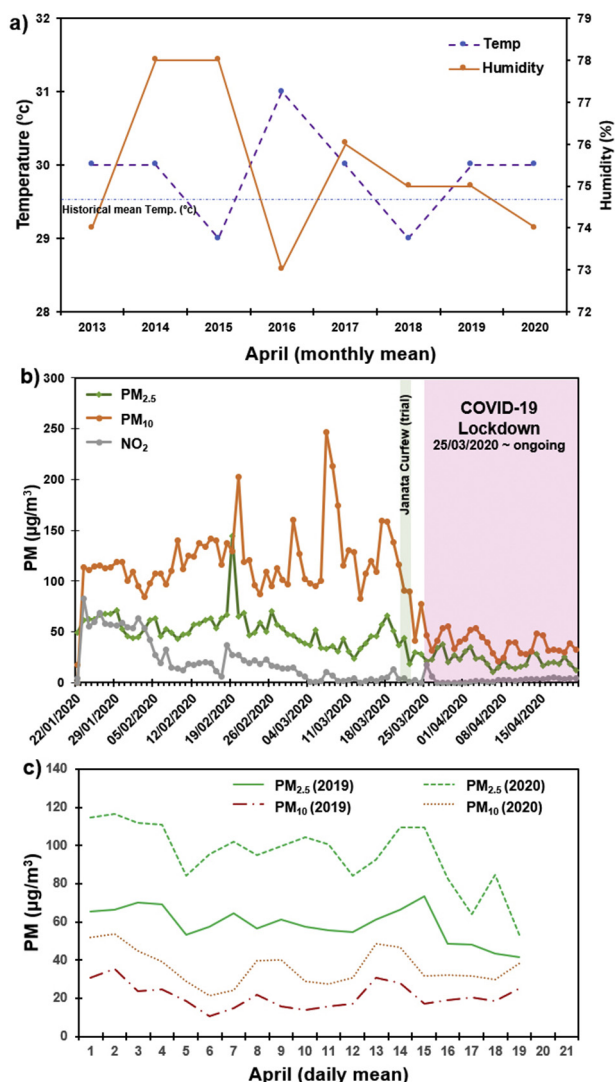
Fig. A2. (a) time-series plot of April month average temperature and humidity for Cochin (9.9312° N, 76.2673° E), (b) PM$_{2.5}$, PM$_{10}$ and NO$_2$ concentration at Vytilla station (9.958233° N 76.325229° E), and (c) comparative plot of April month daily mean PM$_{2.5}$ and PM$_{10}$ for 2019 and 2020 (source: Central and State pollution control board).

References

Akimoto, H., 2003. Global air quality and pollution. Science 302, 1716–1719.
Balchand, A., Nair, S., 1994. Studies on the fractionation of phosphates in the sediments of a tropical water way. Environ. Geol. 23, 284–294.
Caballero, I., Stumpf, R.P., 2019. Retrieval of nearshore bathymetry from sentinel-2A and 2B satellites in South Florida coastal waters. Estuar. Coast. Shelf Sci. 226, 106277.
Clifford, C., 2020. The Water in Venice, Italy's Canals Is Running Clear amid the COVID-19 Lockdown — Take a Look [WWW Document]. URL. https://www.cnbc.com/2020/03/18/photos-water-in-venice-italys-canals-clear-amid-covid-19-lockdown.html, Accessed date: 17 April 2020.
Curran, P., Hansom, J., Plummer, S., Pedley, M., 1987. Multispectral remote sensing of nearshore suspended sediments: a pilot study. Int. J. Remote Sens. 8, 103–112.
Davies-Colley, R., Smith, D., 2001. Turbidity suspended sediment, and water clarity: a review. J. Am. Water Res. Assoc. 37, 1085–1101.
Dogliotti, A.I., Ruddick, K., Nechad, B., Doxaran, D., Knaeps, E., 2015. A single algorithm to retrieve turbidity from remotely-sensed data in all coastal and estuarine waters. Remote Sens. Environ. 156, 157–168.
Doxaran, D., Froidefond, J.-M., Lavender, S., Castaing, P., 2002. Spectral signature of highly turbid waters: application with SPOT data to quantify suspended particulate matter concentrations. Remote Sens. Environ. 81, 149–161.
Doxaran, D., Froidefond, J.-M., Castaing, P., 2003. Remote-sensing reflectance of turbid sediment-dominated waters. Reduction of sediment type variations and changing illumination conditions effects by use of reflectance ratios. Appl. Opt. 42, 2623–2634.

ESA, 2020. COVID-19: nitrogen dioxide over China. [WWW Document]. URL. https://www.esa.int/Applications/Observing_the_Earth/Copernicus/Sentinel-5P/COVID-19_nitrogen_dioxide_over_China, Accessed date: 17 April 2020.
Häder, D.-P., Banaszak, A.T., Villafañe, V.E., Narvarte, M.A., González, R.A., Helbling, E.W., 2020. Anthropogenic pollution of aquatic ecosystems: emerging problems with global implications. Sci. Total Environ. 713, 136586.
Henriques, M., 2020. Will Covid-19 Have a Lasting Impact on the Environment?. [WWW Document]. URL. https://www.bbc.com/future/article/20200326-covid-19-the-impact-of-coronavirus-on-the-environment, Accessed date: 17 April 2020
Luis, K.M., Rheuban, J.E., Kavanaugh, M.T., Glover, D.M., Wei, J., Lee, Z., Doney, S.C., 2019. Capturing coastal water clarity variability with Landsat 8. Mar. Pollut. Bull. 145, 96–104.
Mani, K.S., 2020. The Lockdown Cleaned the Ganga More than 'Namami Gange' Ever Did. [WWW Document]. URL. https://science.thewire.in/environment/ganga-river-lockdown-cleaner-namami-gange-sewage-treatment-ecological-flow/, Accessed date: 19 April 2020.
Masood, N., Zakaria, M.P., Halimoon, N., Aris, A.Z., Magam, S.M., Kannan, N., Mustafa, S., Ali, M.M., Keshavarzifard, M., Vaezzadeh, V., et al., 2016. Anthropogenic waste indicators (AWIs), particularly PAHs and LABs, in Malaysian sediments: application of aquatic environment for identifying anthropogenic pollution. Mar. Pollut. Bull. 102, 160–175.
Mohan, M., Chandran, M.S., Jayasooryan, K., Ramasamy, E., 2014. Mercury in the sediments of Vembanad Lake, western coast of India. Environ. Monit. Assess. 186, 3321–3336.
Narayanan, N., Venot, J.-P., 2009. Drivers of change in fragile environments: Challenges to governance in Indian wetlands. Natural Resources Forum. Wiley Online Library, pp. 320–333.
Nechad, B., Ruddick, K., Park, Y., 2010. Calibration and validation of a generic multisensor algorithm for mapping of total suspended matter in turbid waters. Remote Sens. Environ. 114, 854–866.
Novo, E., Hansom, J., Curran, P., 1989. The effect of viewing geometry and wavelength on the relationship between reflectance and suspended sediment concentration. Int. J. Remote Sens. 10, 1357–1372.
Padmalal, D., Maya, K., Sreebha, S., Sreeja, R., 2008. Environmental effects of river sand mining: a case from the river catchments of Vembanad lake, Southwest coast of India. Environ. Geol. 54, 879–889.
Pahlevan, N., Roger, J.-C., Ahmad, Z., 2017. Revisiting short-wave-infrared (SWIR) bands for atmospheric correction in coastal waters. Opt. Express 25, 6015–6035.
Priju, C., Narayana, A., 2007. Heavy and trace metals in Vembanad Lake sediments. Int. J. Environ. Res. 1, 280–289.
Ramasamy, E., Jayasooryan, K., Chandran, M.S., Mohan, M., 2017. Total and methyl mercury in the water, sediment, and fishes of Vembanad, a tropical backwater system in India. Environ. Monit. Assess. 189, 130.
Ritchie, J.C., Cooper, C.M., Schiebe, F.R., 1990. The relationship of MSS and TM digital data with suspended sediments, chlorophyll, and temperature in Moon Lake, Mississippi. Remote Sens. Environ. 33, 137–148.
Schlacher, T.A., Lucrezi, S., Connolly, R.M., Peterson, C.H., Gilby, B.L., Maslo, B., Olds, A.D., Walker, S.J., Leon, J.X., Huijbers, C.M., et al., 2016. Human threats to sandy beaches: a meta-analysis of ghost crabs illustrates global anthropogenic impacts. Estuar. Coast. Shelf Sci. 169, 56–73.
SCRIPPS, 2020. Research in the time of COVID-19. [WWW Document]. URL. https://scripps.ucsd.edu/news/research-time-covid-19, Accessed date: 17 April 2020.
Song, K., Wang, Z., Blackwell, J., Zhang, B., Li, F., Zhang, Y., Jiang, G., 2011. Water quality monitoring using Landsat Themate Mapper data with empirical algorithms in Chagan Lake, China. J. Appl. Remote Sens. 5, 053506.
Sravanthi, N., Ramana, I., Yunus Ali, P., Ashraf, M., Ali, M., Narayana, A., 2013. An algorithm for estimating suspended sediment concentrations in the coastal waters of India using remotely sensed reflectance and its application to coastal environments. Int. J. Environ. Res. 7, 841–850.
Sruthy, S., Ramasamy, E., 2017. Microplastic pollution in Vembanad Lake, Kerala, India: the first report of microplastics in lake and estuarine sediments in India. Environ. Pollut. 222, 315–322.
Stone, M., 2020. Carbon emissions are falling sharply due to coronavirus. But not for long. [WWW Document]. URL. https://www.nationalgeographic.com/science/2020/04/coronavirus-causing-carbon-emissions-to-fall-but-not-for-long/, Accessed date: 17 April 2020.
Stumpf, R.P., Pennock, J.R., 1989. Calibration of a general optical equation for remote sensing of suspended sediments in a moderately turbid estuary. J. Geophys. Res. Oceans 94, 14363–14371.
Tassan, S., 1994. Local algorithms using SeaWiFS data for the retrieval of phytoplankton, pigments, suspended sediment, and yellow substance in coastal waters. Appl. Opt. 33, 2369–2378.
Vanhellemont, Q., 2019. Adaptation of the dark spectrum fitting atmospheric correction for aquatic applications of the Landsat and Sentinel-2 archives. Remote Sens. Environ. 225, 175–192.
Vanhellemont, Q., Ruddick, K., 2014. Turbid wakes associated with offshore wind turbines observed with Landsat 8. Remote Sens. Environ. 145, 105–115.
Vanhellemont, Q., Ruddick, K., 2018. Atmospheric correction of metre-scale optical satellite data for inland and coastal water applications. Remote Sens. Environ. 216, 586–597.
Vinita, J., Revichandran, C., Manoj, N., 2017. Suspended sediment dynamics in Cochin estuary, west coast, India. J. Coast. Conserv. 21, 233–244.
Volkamer, R., Jimenez, J.L., San Martini, F., Dzepina, K., Zhang, Q., Salcedo, D., Molina, L.T., Worsnop, D.R., Molina, M.J., 2006. Secondary organic aerosol formation from anthropogenic air pollution: rapid and higher than expected. Geophys. Res. Lett. 33.
Wass, P., Marks, S., Finch, J., Leeks, G.J., [xdot], L., Ingram, J., 1997. Monitoring and preliminary interpretation of in-river turbidity and remote sensed imagery for suspended

sediment transport studies in the Humber catchment. Sci. Total Environ. 194, 263–283.

Wei, J., Lee, Z., Garcia, R., Zoffoli, L., Armstrong, R.A., Shang, Z., Sheldon, P., Chen, R.F., 2018. An assessment of Landsat-8 atmospheric correction schemes and remote sensing reflectance products in coral reefs and coastal turbid waters. Remote Sens. Environ. 215, 18–32.

Woodruff, D.L., Stumpf, R.P., Scope, J.A., Paerl, H.W., 1999. Remote estimation of water clarity in optically complex estuarine waters. Remote Sens. Environ. 68, 41–52.

Worldometers.info, 2020. Coronavirus Updates. [WWW Document]. URL. https://www.worldometers.info/, Accessed date: 18 April 2020.